JOURNAL OF CATALYSIS **178,** 58–65 (1998)
ARTICLE NO. CA982118

The Effect of Sn on the Reactions of *n*-Hexane and Cyclohexane over Polycrystalline Pt Foils

T. Fujikawa,[1] F. H. Ribeiro,[2] and G. A. Somorjai

Department of Chemistry, University of California at Berkeley, Berkeley, California 94720, and Center for Advanced Materials, Materials Sciences Division, E.O. Lawrence Berkeley National Laboratory, Berkeley, California 94720

Received August 18, 1997; revised March 27, 1998; accepted April 27, 1998

The modification of the catalytic properties of a polycrystalline platinum foil by the addition of tin was studied by the reactions of *n*-hexane and cyclohexane in excess H_2. The reactions were studied at 13.3 kPa of *n*-hexane, 450 kPa of H_2 and 740 K, and 6.7 kPa of cyclohexane, 450 kPa of H_2 and 573 K. The Pt–Sn catalyst was characterized by Auger electron spectroscopy and by temperature-programmed desorption of CO before and after the reactions. The sites that bind CO most strongly on the Pt foil also have the highest initial turnover rate and are the first ones to be poisoned by carbon deposits from hydrocarbon reactions or by sulfur when a sulfur-containing compound (thiophene) is present in the feed. The addition of tin can block these sites preferentially, thus decreasing the undesirable high initial hydrogenolysis rate of platinum catalysts in reforming reactions and eliminating the need for presulfiding the catalyst. Also, tin suppressed the hydrogenolysis reaction preferentially to the isomerization and cyclization reactions thus increasing the selectivities to isomerization and cyclization. The amount of carbon deposited was smaller on tin containing platinum catalysts during the dehydrogenation of cyclohexane and *n*-hexane. © 1998 Academic Press

1. INTRODUCTION

Platinum based bimetallic catalysts are extensively used in naphtha reforming processes. The three major bimetallic systems in current use are Pt–Re (1), Pt–Ir (2), and Pt–Sn (3–5). Industrially, Pt–Re and Pt–Ir systems are used for semiregenerative reforming processes (6) or cyclic reforming processes (7). Because the Pt–Sn catalyst can be regenerated easily, it is preferred for low-pressure continuous catalyst regeneration (CCR) reforming processes (8).

The advantages of the addition of Sn to Pt is that it improves the stability of the catalyst by decreasing the rate of carbon deposition, it enhances the yields of C_5^+ reformate and hydrogen by suppressing the hydrogenolysis reaction, and it depresses the high initial rate of the Pt catalyst. The modification of the catalytic properties of Pt has been investigated by many researchers (9–23). The modified catalytic behavior of Pt–Sn catalysts exhibiting improved reforming selectivity and reduced deactivation by coking has been explained by many as an ensemble or a ligand effect. Dautzenberg *et al.* (15) and Biloen *et al.* (24) suggested that the effect of tin is to divide the surface into a smaller number of contiguous platinum atoms and that this arrangement brings about the beneficial effects on the selectivity and stability of the catalysts (ensemble effect). However, Burch and Garla (10) proposed that the role of tin is to modify the electronic properties of the small platinum particles (ligand effect). Another question under discussion is whether the state of the tin atoms in platinum–tin catalysts is in a zero valence or in an oxidized state. Although some researchers reported that tin was present in an oxidized state in platinum–tin catalysts and that the interaction between Pt and Sn^{+2} or Sn^{+4} may be the cause of an increased selectivity and better activity maintenance (9–12, 25–28), other researchers reported that part of the tin was present in a metallic state and alloyed with platinum and that the alloy is responsible for a higher selectivity and increased stability (15, 18–23, 29–31). Much progress has been made in understanding this system, but some issues on the effect of Sn on supported Pt–Sn catalysts are still a matter of debate. The reactions of hydrocarbons on supported catalysts in general are quite complex because of the nature of the interaction of the various components in this system. For example, the performance of the catalyst will depend on the catalyst preparation variables including metal precursors, support, treatments, the reaction conditions under which the test is performed (total and relative pressure and temperature), the nature of the hydrocarbons, and bifunctional reactions to name a few of the parameters. Our approach in studying these complex systems has been to build a model catalyst where a particular part of this system can be studied. For example, in this present study, we directly investigate the metal–metal interaction between platinum and tin in the

[1] Permanent address: Cosmo Research Institute, Research and Development Center, 1134-2, Gongendo, Satte-shi, Saitama 340-0193, Japan.

[2] To whom correspondence should be addressed. Permanent address: Worcester Polytechnic Institute, Department of Chemical Engineering, Worcester, MA 01609-2280.

0021-9517/98 $25.00

absence of the alumina support. We performed surface science and reaction studies on model Pt–Sn catalysts with a small surface area ($\sim$1 cm^2) sample in the same way as in our previous studies of Pt–Re (32, 33) and Pt–Ir (34) catalysts. We have used a foil in this study to be able to introduce step sites as opposed to the smooth single crystal ordered alloys that can be formed in this system (see, for example, Refs. 35–37). We will report catalytic studies on this ordered alloy in a forthcoming publication (38). The reaction of *n*-hexane conversion and cyclohexane dehydrogenation were performed at a total pressure of 450 kPa, which is close to the commercial reaction pressure of CCR processes. The temperature-programmed desorption (TPD) of CO was used to titrate the number of bare platinum sites, and Auger electron spectroscopy (AES) was used to obtain the composition of the catalyst surface before and after reaction. Our conclusion is that Sn is functionally equivalent to sulfur (site-blocker) but because Sn remains on the Pt catalyst after the regeneration process, a Pt–Sn catalyst in a commercial CCR unit can be put back on stream without a presulfidation step.

2. EXPERIMENTAL METHODS

2.1. Apparatus

All the experiments were performed in a stainless steel ultrahigh-vacuum (UHV) chamber (base pressure 8×10^{-10} Torr) equipped with an AES retarding field analyzer, a UTI 100C quadrupole mass spectrometer, a metal deposition source, and a retractable internal isolation cell for high pressure (450 kPa) catalytic reactions. This UHV surface analysis/high-pressure catalytic reaction system has been described in detail in a previous publication (39).

2.2. Preparation of Catalysts

The platinum sample was a $0.71 \times 0.71 \times 0.0076$ cm polycrystalline platinum foil with a purity of 99.95%. It was spot-welded to platinum wires (0.51 mm diameter) which were spot-welded to gold wires (0.71 mm diameter) and then screwed into a copper block in a rotatable manipulator.

The temperature was maintained constant by a temperature controller, and it was measured with a chromel–alumel thermocouple spot welded to the edge of the foil. The sample was cleaned using cycles of oxygen treatment at 900 K and 1×10^{-7} Torr, Ar ion sputtering at room temperature, 5×10^{-5} Torr, and 2-keV ions, and final annealing at 1000 K until the surface impurities such as Ca, Si, S, O, and C could not be detected by AES.

Bimetallic surfaces were prepared by depositing tin on platinum foil in UHV with a pulsed Metal Vapor Vacuum Arc plasma gun (MEVVA). The MEVVA source has been described in detail elsewhere (40, 41). In this study, we used a straight or a curved MEEVA source. The curved design could filter out any nonionic species but had a much lower deposition rate. The straight type was used on the *n*-hexane studies, and the curved type was used on cyclohexane dehydrogenation. After tin deposition, the foil was annealed at 1000 K for 15 s allowing tin to vaporize or diffuse into the bulk. The sample composition was stable after this treatment as confirmed by comparison of the Auger spectra before and after reaction. The 1000 K heating for 15 s was similar to the procedure used to obtain a stable ordered structure of Sn on Pt(111) [see, for example, Paffett and Windham (35)]. In this ordered structure, Sn is incorporated into the Pt surface forming a true alloy. The decrease of the fraction of tin on the platinum surface by the annealing treatment was followed by AES and CO TPD.

2.3. Characterization of Catalysts

AES and TPD of CO were measured before and after each catalytic reaction. The TPD of CO was measured to investigate the platinum distribution on the sample surface as in previous work (42, 43). For the titration of the bare platinum surface by CO adsorption, the sample was flashed up to 673 K in order to desorb adsorbed molecules, and then it was exposed to 50 L (1 L $= 1 \times 10^{-6}$ Torr s) of CO at 300 K. Thermal desorption spectra (TDS) were measured with the mass spectrometer tuned at mass 28, upon heating the foil to 673 K at a rate of 23 K s^{-1}. The amount of adsorbed CO was calculated from the desorption peak area.

The TPD of CO and surface composition after reaction were measured as follows. After reaction, the reaction loop was evacuated by a diffusion pump at room temperature and the high-pressure cell was opened to the UHV chamber. With a pressure of about 1×10^{-8} Torr, the sample was flashed to 673 K, 50 L of CO exposed at room temperature, followed by CO TPD. AES was measured after the CO TPD.

2.4. Turnover Rate Measurements

The turnover rates for *n*-hexane and cyclohexane reactions were measured in a batch reactor (reactor volume of 460 cm^3). After tin deposition and annealing, measurement of surface composition by AES and TPD of CO, the sample was enclosed in the high-pressure cell. Reaction studies of *n*-hexane were carried out under 13.3 kPa of *n*-hexane (Fluka puriss grade), 450 kPa of H_2 at 740 K and cyclohexane at 6.7 kPa of cyclohexane (Fluka puriss grade), 450 kPa of H_2 at 573 K. To investigate the effect of sulfur on the reaction studies of *n*-hexane, 10 ppm of thiophene was added to the feed. The product analysis was performed by on-line gas chromatography (Hewlett-Packard 5890-II) equipped with a flame ionization detector and a capillary column (Pona, 50 m, 0.2 mm diameter). The first analysis was performed after 3 min of reaction and subsequent analyses were carried out at intervals of 15 min, for a total time of about

100 min. In this paper, the rates were described as nominal turnover rates and turnover rates. The nominal turnover rates were calculated assuming that all surface atoms were active (1×10^{15} atoms cm^{-2}) (44). The turnover rates were calculated based on the number of surface platinum atoms as measured by CO TPD.

3. RESULTS AND DISCUSSION

3.1. Temperature-Programmed Desorption of CO

Temperature-programmed desorption of CO was used to measure the number and type of Pt surface atoms. The CO TPD from the clean platinum foil is shown in Fig. 1. The two peaks with maximum at about 430 K and 540 K were deconvoluted assuming first-order desorption, and the simplified equation developed by Redhead (45). The peak areas are in the ratio of 1 to 2. The TPD spectra of CO from a platinum foil measured by Collins *et al.* (46, 47) is in agreement with our work. They found two distinct desorption states with peaks at about 440 K and 550 K from a Pt foil annealed at 1112 K in O_2 and the same area ratio for the two desorption peaks. The origin of the two peaks can be rationalized by comparing our data with the CO desorption data on Pt(111) (47), Pt(335) (48, 49), Pt(112) (49), and Pt(113) (50) single crystals. These single-crystal surfaces consist of (111) terraces with a width of four, three, and two atoms respectively for Pt(335), Pt(112) and Pt(113). The terraces are separated by steps of (100) orientation. The CO TPD on Pt(111) shows only one peak at about 430 K with a saturation coverage of 0.5 ML (47). For the Pt(335), Pt(112), and Pt(113), where step atoms are present with different densities, there are two peaks at about the same desorption temperature as for the Pt foil in our work. The area in the low temperature peak is proportional to the amount of atoms on the (111) terrace and the area in the higher temperature peak is proportional to the amount of atoms on the steps (48, 49). The saturation CO coverage for Pt(111), Pt(335), Pt(112) and Pt(113) is 0.5, 0.60, 0.63 and 0.75 respectively which corresponds to a stoichiometry of two Pt atoms for each CO on the (111) terrace and one Pt atom for each CO on the step. We can then conclude from the relative areas in the TPD that the Pt foil used in this study had half of the atoms as Pt(111) and the other half as steps. This results is reasonable in view of the low annealing temperature (1000 K) that the foil was subjected to after argon sputtering. Higher annealing temperatures (1700 K) of the foil will produce mostly (111) planes (47).

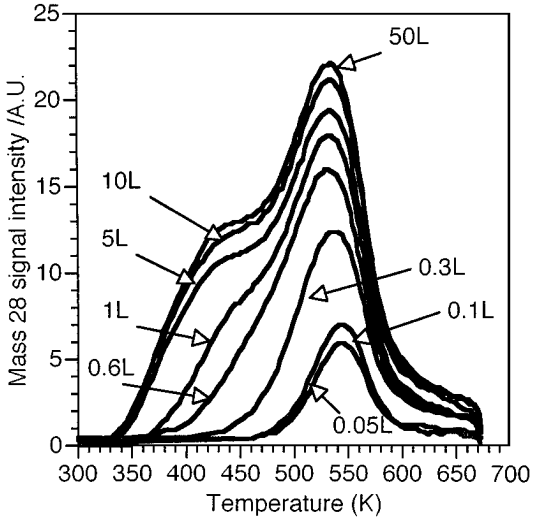

FIG. 1. CO TPD on a Pt foil with exposure from 0.05 to 50 L. Adsorption temperature 300 K, and heating rate 15 K s^{-1}.

The TPD spectra of CO from a platinum foil as a function of the amount of Sn before and after cyclohexane dehydrogenation is shown in Fig. 2. The higher temperature peak disappears by adding Sn (Fig. 2A), which indicates that Sn binds preferentially to the step sites. For the Pt foil with no Sn added, the higher temperature peak also disappears after reaction (Fig. 2B). Thus, carbon also selectively deposits on the step platinum sites. Davis *et al.* (42) also investigated the CO desorption spectra (exposure = 36 L) for the flat (111) platinum surface and the stepped (13,1,1) platinum surface before and after reaction of *n*-hexane. The CO desorption spectra for the (111) platinum surface has a peak in the low-temperature range, which is at about 430 K. However, CO thermal desorption spectra for the (13,1,1) platinum surface has two or more overlapping desorption peaks, the most prominent of which displayed a desorption peak maximum at 560 K. Their data also indicated that the higher peak disappears after reaction. It was concluded that the (111) sites on the terraces are tolerant to deactivation by carbonaceous deposits.

It is concluded from Fig. 2 that Sn covers preferentially the platinum sites that will also be covered preferentially by carbonaceous deposits. Thus, the effects of tin and carbon for the desorption of CO seem to be the same. Palazov *et al.* (51) previously proposed that deposited coke and tin block the same active sites on the platinum surfaces based on the IR data of chemisorbed CO. Biloen *et al.* (24) suggested that sulfur, carbon, tin, gold, and many other catalytically inert modifiers act in the same way as rhenium–sulfur, which divides the platinum surface into small ensembles. In this study, the CO TPD with preadsorbed sulfur (not shown) did not show the same effect as Sn and carbon but the Pt surface still showed the high binding temperature peak on the CO TPD with adsorbed sulfur. This result surprised us because we expected that S and Sn would adsorb on the same high-energy sites. For example, Kiskinova *et al.* (52) found that sulfur affects first the high-energy adsorption sites of Pt(111). In addition, as we will show later, the sulfur-covered surface was catalytically similar to the surface with Sn.

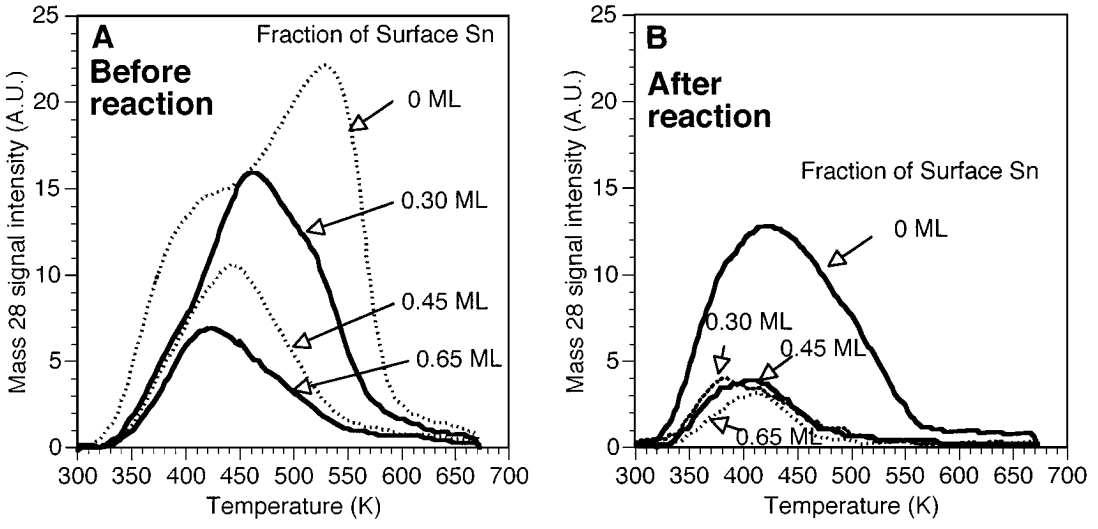

FIG. 2. CO TPD on a Sn-covered Pt foil before (A) and after (B) cyclohexane reaction as a function of the fraction of surface Sn in monolayers (ML). Adsorption temperature 300 K, CO exposure 50 L, and heating rate 15 K s^{-1}. Reaction conditions: 6.7 kPa of cyclohexane, 450 kPa of H_2, and 573 K.

3.2 Surface Composition of the Pt–Sn Bimetallic System

The fraction of tin on the surface of the foil after annealing was determined by CO TPD and by AES (Fig. 3). In general, the variation of the amount of tin on the surface as a function of Sn deposited show the same trend by CO TPD and AES. Also, the two different types of deposition gun produce a similar curve shape and maximum uptake (Figs. 3A, B).

The data in Fig. 3 suggest that the amount of Sn reaches a saturation level, as is well documented in the literature for single crystals (35). On the very well-characterized Sn/Pt(111) system, it has been shown (35, 53) that Sn will form a true alloy with Pt and will be incorporated into the Pt surface. We expect the same behavior for a Pt foil because it is composed manly of Pt(111) planes with defects. The Pt–Sn bond is stronger than the Pt-Pt and Sn-Sn bond and Sn will tend to form an alloy with Pt, sometimes diffusing into the bulk. For example, on a Pt(111) surface, there is a maximum coverage of surface Sn that can be obtained (about 0.33 monolayer). Any additional amount of Sn that is added to the surface either evaporates or diffuses into the bulk upon annealing, leaving the surface at a maximum 0.33 ML coverage on the Pt(111) surface. This high affinity

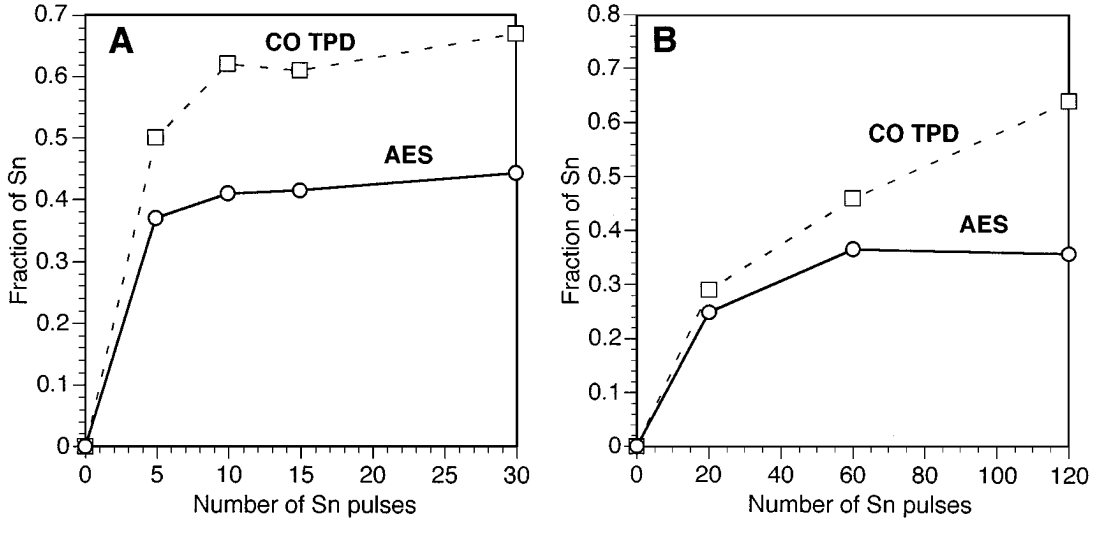

FIG. 3. Fraction of Sn on the surface as a function of the plasma gun pulses as determined by AES and CO TPD. (A) Plasma gun without ion filter. (B) Plasma gun with ion filter.

of Sn to Pt and the low Sn vapor pressure contribute to the depletion of Sn on the surface when it is annealed, and thus the final amount of tin will be different from the amount initially deposited on the surface. Note, however, that the saturation of Sn depends on the single crystal surface. For example, the Pt coverage will be 0.5 ML for $Pt_3Sn(100)$ but 0.7 ML for $Pt_3Sn(111)$ (54). In the case of a foil, the saturation value should vary depending on the density of defects, where Sn may have a higher affinity to bind, and on the density of the different faces exposed.

To calculate the coverage by AES, after the surface is annealed, the signal was corrected with the published relative signals of Pt 237 eV and Sn 430 eV peaks (55). Note, however, that the amount of Sn may be overestimated from the contribution of subsurface Sn as a consequence of the diffusion of Sn into the bulk.

The amount of CO desorbed on the TPD experiment was also used to calculate the amount of Pt. This method of calculation has a few shortcomings to be discussed in turn. The amount of CO adsorbed may not be proportional to the amount of Pt on the surface if Sn affects the binding properties of Pt atoms adjacent to it. The current literature does not agree on this point: Paffett *et al.* (56) working on ordered Sn alloys on Pt(111) found that Sn acts as less than a 1 : 1 site blocker (Sn blocks less than 1 CO site per Sn atom), whereas Haner *et al.* (54) reported that on a Pt_3Sn single crystal Sn acted as a 1 : 1 site blocker. Another possible problem is that as Sn is adsorbed on the defects of the foil, the overall stoichiometry for CO adsorption may change [1 CO to 1 Pt on steps and 1 CO to 2 Pt on (111) faces].

From these discussions, there are pitfalls in the determination of the actual amount of surface Pt from AES or TPD methods. We will use CO TPD to count the number of sites because this technique was the more sensitive. Note, however, that this approximate estimate of coverage is accurate enough for the conclusions in this work.

3.3. *Conversion of n-Hexane over Pt–Sn*

Reaction studies of the conversion of *n*-hexane were performed on the tin-covered platinum foil. The reaction products analyzed by the gas chromatograph were $C_{1\text{-}5}$ hydrocarbons, 1-hexene, 2-methylpentane, 3-methylpentane, and methylcyclopentane. The dehydrocyclization of *n*-hexane to form benzene was not observed. The nominal number of turnovers (number of molecules formed per total number of surface atoms) versus time plot for the reaction of *n*-hexane is shown for the Pt foil (Fig. 4A) and for the foil after 30 pulses of Sn (Fig. 4B) (about 0.6 ML of tin by CO TPD). Note that there is a larger decrease of the number of turnovers as a function of time for the model catalysts than it is normally observed on supported catalysts. The reason for the larger decrease in our system may be that the samples are pristine before reaction, exposing high activity sites (step sites) that are quickly poisoned under reaction conditions. For the supported catalysts, most of these sites are probably poisoned before the reaction even starts (from impurities adsorbed during the preparation of the catalyst) and thus the initial drop in activity, although still severe for a monometallic Pt catalysts, is not as steep as observed here. There is less deactivation for the sample with Sn (less curvature on the lines), but the major difference is the decrease in the initial rate of hydrogenolysis when tin is added. This fact can also be illustrated in Fig. 5 for the conversion of *n*-hexane as a function of the amount of tin on the surface. Tin decreases the hydrogenolysis rate most strongly with a

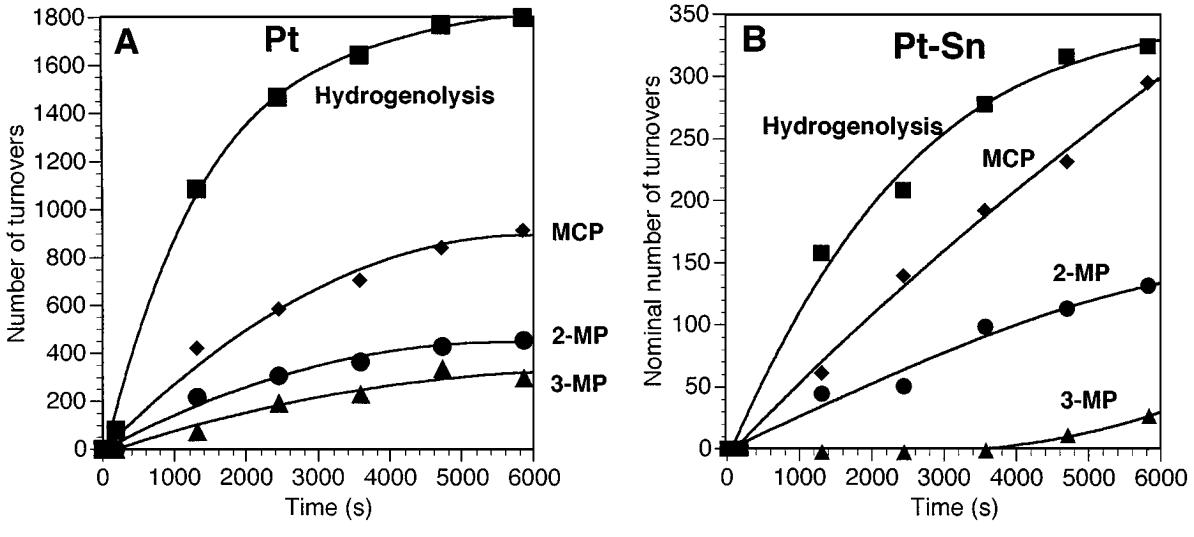

FIG. 4. Number of *n*-hexane molecules converted to products per total surface atom (number of turnovers) as a function of time: (A) no Sn, (B) 30 pulses Sn (about 0.6 ML of Sn). Reaction conditions: 13.3 kPa of *n*-hexane, 450 kPa of H_2, and 740 K.

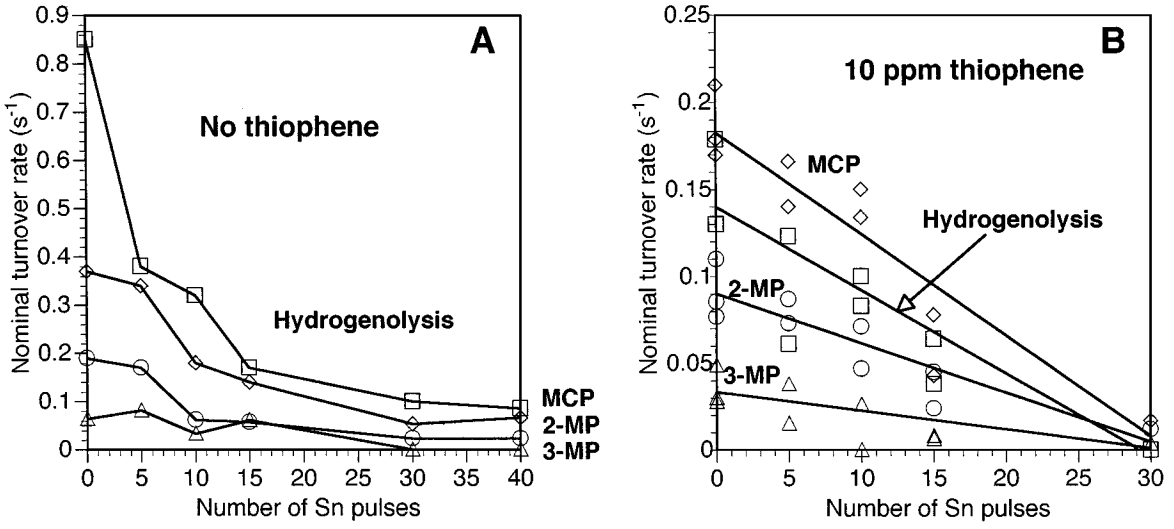

FIG. 5. Nominal turnover rate as a function of deposited tin. (A) No sulfur compounds added. (B) 10 ppm of thiophene added. Reaction conditions: 13.3 kPa of *n*-hexane, 450 kPa of H_2, and 800 K.

smaller decrease for the isomerization and cyclization rates as compared to the platinum mono-metallic catalyst. Thus, selectivity to isomerization and cyclization are increased by the addition of tin. It is interesting to note that most of the drop in hydrogenolysis rates occurs after the addition of 0.5 ML (5 pulses of Sn), which is sufficient to cover the step sites while the isomerization and cyclyzation reactions hardly change at this Sn surface concentration. Although we do not have intermediate measurements between the pure Pt foil and 0.5 ML of Sn, this result suggests that tin inhibits the sites (step sites) responsible for hydrogenolysis before it affects the sites responsible for isomerization and cyclization [Pt(111)]. Note also in Fig. 5A that there is a gradual decrease in all the rates as a function of Sn content which parallels the changes in Fig. 3 for CO TPD and AES.

To study the effect of sulfur, an ever-present contaminant in real feedstocks, 10 ppm of thiophene was added to the *n*-hexane feed (Fig. 5B). Now, all the catalysts are in the same trend line including the monometallic Pt foil. Sulfur thus decreases the rate on the Pt foil in a similar way to Sn. The effect of sulfur (Fig. 5B) can be studied by comparing the results with the runs without sulfur (Fig. 5A). The same products are observed, but all the rates are lower. In particular, the hydrogenolysis rate decrease on the Pt foil (with no Sn) more rapidly than the isomerization rates, thus changing the initial product distribution. Note, however, that on the Pt–Sn samples, the hydrogenolysis rate had already been depressed by the Sn, and the addition of sulfur just decreases all the rates equally. Another observation was that although sulfur was detected on the clean Pt foil after reaction, when tin was added to the foil, no sulfur could be detected after reaction. Sulfur and Sn probably adsorb preferentially on the step sites, which are also the sites with high rates of hydrogenolysis. When Sn is already present on the step sites, sulfur is adsorbed only at the (111) sites and cannot stay on the surface in high concentration under reaction conditions. These results suggest that tin competes with sulfur for adsorption on platinum.

Tin decreases the initial high rates for the hydrogenolysis reaction. Because the hydrogenolysis reaction is exothermic, the initial industrial operation of reforming can exhibit a steep rising temperature and damage the catalyst and reactor. Thus, in the case of commercial semi-regenerative and cyclic reforming processes, the catalyst is pre-sulfided after the coke burning regeneration to avoid this high initial hydrogenolysis activity (57) as sulfur selectively reduces the hydrogenolysis reaction on reforming catalysts. However, in the case of CCR processes, the sulfur pretreatment after coke burning is not necessary because tin plays a role similar to sulfur in poisoning the sites responsible for hydrogenolysis.

3.4. Dehydrogenation of Cyclohexane over Pt–Sn

The dehydrogenation of cyclohexane was also studied as a model for the reforming reactions. The only product observed was benzene. The product accumulation plots are shown in Fig. 6. Again, there is a rapid initial deactivation as in the case of *n*-hexane. The evident effect of Sn is to tone down the high initial activity of pure platinum catalysts. It is not evident from these experiments, however, that, after the initial deactivation, Pt–Sn is more stable than Pt.

The initial turnover rates, based on the number of Pt surface atoms counted by CO TPD, is shown in Fig. 7. It is well established that tin acts as a poison and thus the rate per gram of a Pt catalyst will be decreased by the addition

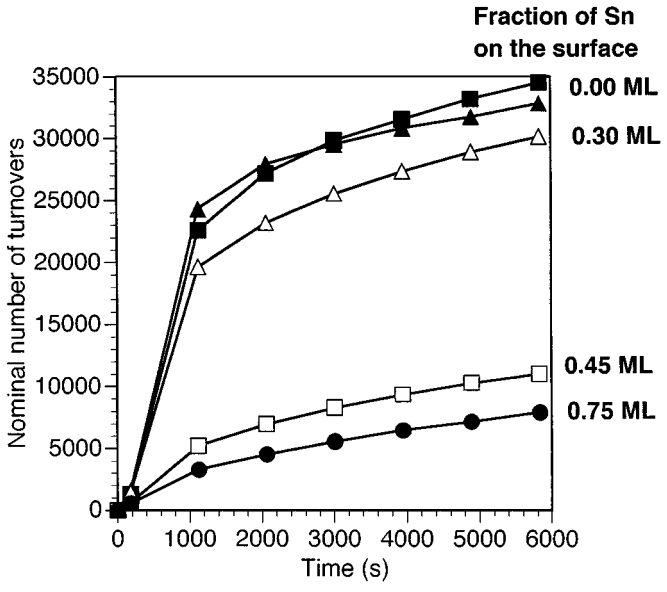

FIG. 6. Number of cyclohexane molecules converted to benzene per total surface atom as a function of time on a platinum foil with various amounts of deposited tin. Reaction conditions: 6.7 kPa of cyclohexane, 450 kPa of H_2, and 573 K.

of Sn for cyclohexane dehydrogenation (11, 58). However, because this is a structure-insensitive reaction (59, 60), the turnover rate should be constant regardless of the amount of tin. In agreement with this work, Cortright and Dumesic (61) also found that the turnover rate decreased for the dehydrogenation of isobutane by the addition of Sn.

The final turnover rates, based on the number of Pt surface atoms counted by CO TPD *after reaction* were also measured. Again, the turnover rates were not constant as

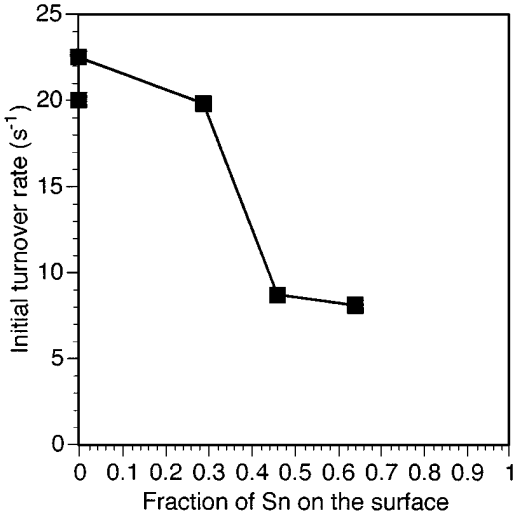

FIG. 7. Initial turnover rate for cyclohexane dehydrogenation on a Pt foil as a function of the fraction of Sn. The number of Pt atoms on the surface were counted by CO TPD. Reaction conditions: 6.7 kPa of cyclohexane, 450 kPa of H_2, and 573 K.

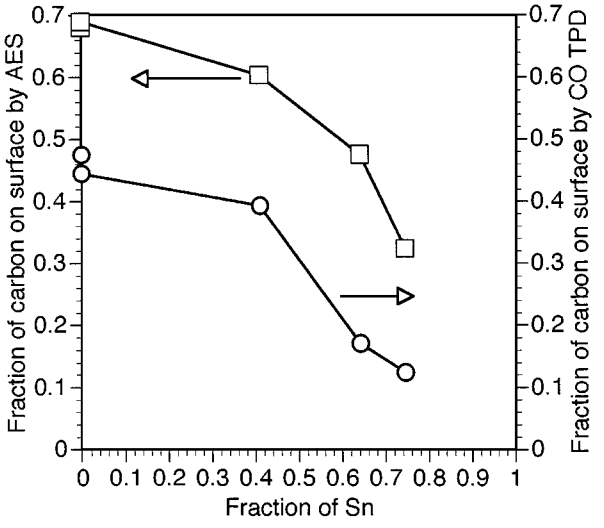

FIG. 8. Fraction of carbon on the surface after cyclohexane reaction (6.7 kPa of cyclohexane, 450 kPa of H_2, 573 K, and 6 ks) as a function of Sn on the Pt foil. Fraction of carbon measured by AES and by CO TPD.

expected for a structure-insensitive reaction, and, in this case, they showed a maximum. The final turnover rates were also not the same as the initial rates. The values for the final turnover rates are a factor of 2 lower than the initial rates, except for Pt where the turnover rates decreased by a factor of 10. This difference may be the result of the interference of adsorbed carbon with the adsorption of CO at the low exposures used in this work.

3.5. Amount of Carbon after Reaction

The amount of carbon after the reaction of cyclohexane dehydrogenation was investigated by AES and CO TPD (Fig. 8). The curve shapes are similar with both techniques. It is clear that tin decreases the carbon deposition rate. The amount of carbon deposited was also investigated after the *n*-hexane reaction, with a similar decrease in the amount of carbon as Sn was added to Pt.

4. CONCLUSIONS

The main conclusion of this work is that Sn (0.5 monolayers) tones down the high initial rate of hydrogenolysis present on Pt catalysts without affecting significantly the rates of isomerization and cyclization. Tin does that by binding preferentially to the step sites which are the ones with the highest activity for hydrogenolysis. In this way, Sn behaves like sulfur in depressing the high initial hydrogenolysis activity in Pt catalysts. The monometallic Pt catalysts deactivate very quickly at the beginning of the reaction because of carbon deposition but then the rate of deactivation is similar to the one on Pt–Sn catalysts for the cyclohexane reaction. Thus, deposited carbon also blocks the high hydrogenolysis activity step sites on Pt, which is similar to

the effect of Sn. The amount of carbon after reaction was smaller on Pt–Sn catalysts, however, which indicates that most of the carbon in our experiments is deposited on Pt step sites during the initial high activity period. In an industrial setting, the advantage of Pt–Sn catalyst over, for example, Pt–Re–S seems to be that Pt–Sn can be placed on stream without a careful sulfidation step after regeneration because Sn will be equivalent to sulfur in depressing the undesirable high initial hydrogenolysis activity.

ACKNOWLEDGMENTS

This work was supported by the Director, Office of Energy Research, Office of Basic Energy Sciences, Materials Sciences Division, of the US Department of Energy under contract No. DE-AC03-76SF00098. One of us (T. Fujikawa) acknowledges the financial support from Japan Cooperation Center for Petroleum Industry Development (JCCP) and Cosmo Oil Co., Ltd. We thank one of the reviewers for pointing us to a reference for the effect of sulfur on CO adsorption.

REFERENCES

1. Kluksdahl, H. E., US patent 3,415,737 (1968).
2. Sinfelt, J. H., US patent 3,953,368 (1976).
3. Dautzenberg, F. M., German Offenlegungsschrift patent 2,121,765 (1971).
4. Dautzenberg, F. M., and Kouwenkoven, H. W., German Offenlegungsschrift patent 2,153,891 (1972).
5. Wilhelm, F. C., US patent 3,844,938 (1974).
6. Nevison, J. A., Obaditch, C. J., and Dalson, M. H., *Hydrocarb. Process.* **53**, 111 (1974).
7. Stuckey, A. N., Jr., and Bauman, R. F., *Hydrocarb. Process.* **50**, 106 (1971).
8. Sutton, E. A., Greenwood, A. R., and Adams, F. H., *Oil Gas J.* **70**, 52 (1972).
9. Burch, R., *J. Catal.* **71**, 348 (1981).
10. Burch, R., and Garla, L. C., *J. Catal.* **71**, 360 (1981).
11. Sexton, B. A., Hughes, A. E., and Foger, K., *J. Catal.* **88**, 466 (1984).
12. Balakrishnan, K., and Schwank, J., *J. Catal.* **127**, 287 (1991).
13. Balakrishnan, K., and Schwank, J., *J. Catal.* **138**, 491 (1992).
14. Zhou, Y., and Davis, S. M., *Catal. Lett.* **15**, 51 (1992).
15. Dautzenberg, F. M., Helle, J. N., Biloen, P., and Sachtler, W. M. H., *J. Catal.* **63**, 119 (1980).
16. Bacaud, R., Bussiere, P., and Figueras, F., *J. Catal.* **69**, 399 (1981).
17. Lieske, H., and Völter, J., *J. Catal.* **90**, 96 (1984).
18. Kuznetsov, V. I., Belyi, A. S., Yurchenko, E. N., and Smolikov, M. D., *J. Catal.* **99**, 159 (1986).
19. Srinivasan, R., De Angelis, R. J., and Davis, B. H., *J. Catal.* **106**, 449 (1987).
20. Srinivasan, R., De Angelis, R. J., and Davis, B. H., *Catal Lett.* **4**, 303 (1990).
21. Li, Y. X., Stencel, J. M., and Davis, B. H., *Appl. Catal.* **64**, 71 (1990).
22. Srinivasan, R., Rice, L., and Davis, B. H., *J. Catal.* **129**, 257 (1991).
23. Li, Y. X., Klabunde, K. J., and Davis, B. H., *J. Catal.* **128**, 1 (1991).
24. Biloen, P., Helle, J. N., Verbeek, H., Dautzenberg, F. M., and Sachtler, W. M. H., *J. Catal.* **63**, 112 (1980).
25. Adkins, S. R., and Davis, B. H., *J. Catal.* **89**, 371 (1984).
26. Yang, W., Lin, L., Fan, Y., and Zhang, J., *Catal. Lett.* **12**, 267 (1992).
27. Gault, F. G., Zahraa, O., Dartigues, J. M., Maire, G., Peyrot, M., Weisang, E., and Engelhardt, P. A., *in* "Proceedings 7th International Congress on Catalysis, Tokyo, 1980" (T. Seiyama and K. Tanabe, Eds.), Vol. A, p. 199. Elsevier, Amsterdam, 1981.
28. Muller, A. C., Engelhard, P. A., and Weisang, J. E., *J. Catal.* **56**, 65 (1979).
29. Srinivasan, R., and Davis, B. H., *Platinum Met. Rev.* **36**, 151 (1992).
30. Srinivasan, R., and Davis, B. H., *Appl. Catal. A* **87**, 45 (1992).
31. Rajeshwer, D., Basrur, A. G., Gokak, D. T., and Krishnamurthy, K. R., *J. Catal.* **150**, 135 (1994).
32. Ribeiro, F. H., Bonivardi, A. L., and Somorjai, G. A., *Catal. Lett.* **27**, 1 (1994).
33. Ribeiro, F. H., Bonivardi, A. L., Kim, C., and Somorjai, G. A., *J. Catal.* **150**, 186 (1994).
34. Bonivardi, A. L., Ribeiro, F. H., and Somorjai, G. A., *J. Catal.* **160**, 269 (1996).
35. Paffett, M. T., and Windham, R. G., *Surf. Sci.* **208**, 34 (1989).
36. Szanyi, J., Anderson, S., and Paffett, M. T., *J. Catal.* **149**, 438 (1994).
37. Tsai, Y.-L., and Koel, B. E., *J. Phys. Chem. B* **101**, 2895 (1997).
38. Park, Y. K., Ribeiro, F. H., and Somorjai, G. A., *J. Catal.* **178**, 66 (1998).
39. Blakely, D. W., Kozak, E. I., Sexton, B. A., and Somorjai, G. A., *J. Vac. Sci. Technol.* **13**, 1091 (1976).
40. Kim, C., Ogletree, D. F., Salmeron, M. B., Godechot, Y., Somorjai, G. A., and Brown, I. G., *Appl. Surf. Sci.* **59**, 261 (1992).
41. Kim, C., and Somorjai, G. A., *J. Catal.* **134**, 179 (1992).
42. Davis, S. M., Zaera, F., and Somorjai, G. A., *J. Catal.* **77**, 439 (1982).
43. Sachtler, J. W. A., and Somorjai, G. A., *J. Catal.* **81**, 77 (1983).
44. Somorjai, G. A., *in* "Introduction to Surface Chemistry and Catalysis." Wiley, New York, 1994.
45. Redhead, P. A., *Vacuum* **12**, 203 (1962).
46. Collins, D. M., Lee, J. B., and Spicer, W. E., *Surf. Sci.* **55**, 389 (1976).
47. Collins, D. M., and Spicer, W. E., *Surf. Sci.* **69**, 85 (1977).
48. Luo, J. S., Tobin, R. G., Lambert, D. K., Fisher, G. B., and DiMaggio, C. L., *Surf. Sci.* **274**, 53 (1992).
49. Xu, J., and Yates, J. T., Jr., *Surf. Sci.* **327**, 193 (1995).
50. Yamanaka, T., and Matsushima, T., *Shokubai (Catalyst)* **37**, 532 (1995).
51. Palazov, A., Bonev, C., Shopov, D., Lietz, G., Sarkany, A., and Völter, J., *J. Catal.* **103**, 249 (1987).
52. Kiskinova, M., Szabo, A., and Yates, J. T., *J. Chem. Phys.* **89**, 7599 (1988).
53. Overbury, S. H., Mullins, D. R., Paffett, M. T., and Koel, B. E., *Surf. Sci.* **254**, 45 (1991).
54. Haner, A. H., Ross, P. N., Bardi, U., and Atrei, A., *J. Vac. Sci. Technol. A* **10**, 2718 (1992).
55. Palmberg, P. W., Riach, G. E., Weber, R. E., and MacDonald, N. C., *in* "Handbook of Auger Electron Spectroscopy." Physical Electronics Industries, Edina, Minnesota, 1972.
56. Paffett, M. T., Gebhard, S. C., Windham, R. G., and Koel, B. E., *J. Phys. Chem.* **94**, 6831 (1990).
57. Satterfield, C. N., *in* "Heterogeneous Catalysis in Industrial Practice." MacGraw-Hill, New York, 1991.
58. Völter, J., Lietz, G., Uhlemann, M., and Hermann, M., *J. Catal.* **68**, 42 (1981).
59. Boudart, M., *Adv. Catal.* **20**, 153 (1969).
60. Biloen, P., Dautzenberg, F. M., and Sachtler, W. M. H., *J. Catal.* **50**, 77 (1977).
61. Cortright, R. D., and Dumesic, J. A., *J. Catal.* **148**, 771 (1994).